

# Generation of a Stand-Alone Tryptophan Synthase $\alpha$ -Subunit by Mimicking an Evolutionary Blueprint

Michael Schupfner,<sup>[a]</sup> Florian Busch,<sup>[b]</sup> Vicki H. Wysocki,<sup>[b]</sup> and Reinhard Sterner<sup>\*[a]</sup>

The  $\alpha\beta\beta\alpha$  tryptophan synthase (TS), which is part of primary metabolism, is a paradigm for allosteric communication in multi-enzyme complexes. In particular, the intrinsically low catalytic activity of the  $\alpha$ -subunit TrpA is stimulated several hundredfold through the interaction with the  $\beta$ -subunit TrpB1. The BX1 protein from *Zea mays* (zmBX1), which is part of secondary metabolism, catalyzes the same reaction as that of its homologue TrpA, but with high activity in the absence of an interaction partner. The intrinsic activity of TrpA can be significantly increased through the exchange of several active-site loop residues, which mimic the corresponding loop in zmBX1. The subsequent identification of activating amino acids in the generated “stand-alone” TrpA contributes to an understanding of allostery in TS. Moreover, findings suggest an evolutionary trajectory that describes the transition from a primary metabolic enzyme regulated by an interaction partner to a self-reliant, stand-alone, secondary metabolic enzyme.

Allosteric communication is a central mechanism for the regulation of protein-based biological systems. A well-characterized model system for studies on allosteric communication within enzymes is the tryptophan synthase (TS). The TS, an  $\alpha\beta\beta\alpha$  hetero-tetrameric complex that is crucial for primary metabolism in archaea, bacteria, and plants,<sup>[1]</sup> consists of a central dimer of  $\beta$ -subunits (TrpB1) and two peripheral  $\alpha$ -subunits (TrpA). TrpA catalyzes the cleavage of indole-3-glycerol phosphate (IGP) into glyceraldehyde 3-phosphate (GAP) and indole. The latter is channeled to the active site of TrpB1, where the cofactor pyridoxal-5'-phosphate (PLP) facilitates its condensation with L-serine to the final product L-tryptophan.<sup>[2]</sup> TrpA and TrpB1 mutually stimulate each other (Figure 1A), but the underlying allosteric pathways are not fully understood. Recently, a partial comprehension of the activation of TrpB1 by TrpA was achieved through directed evolution towards a “stand-alone” TrpB1 subunit, which contained amino acid exchanges that mimicked its stimulation by TrpA in wild-type TS.<sup>[3]</sup>


Interestingly, a blueprint for a stand-alone TrpA protein already exists in nature. This protein is named BX1 and is a pa-

ralogue of TrpA that plays a role within the secondary metabolism of, for example, plants such as *Zea mays*. BX1 shares with TrpA the ubiquitously encountered  $(\beta\alpha)_8$ -barrel fold,<sup>[4]</sup> and the enzyme from *Z. mays* (zmBX1) shares a sequence identity of 63.3% with zmTrpA (Figure S1 in the Supporting Information). Remarkably, BX1 catalyzes the same IGP lyase reaction as TrpA (Figure 1A) by using identical active site residues,<sup>[5]</sup> but with high efficiency in the absence of an interaction partner.<sup>[6]</sup> Indole generated by BX1 is not used for tryptophan biosynthesis, but is fed into the benzoxazinoid pathway, where it is finally converted into the plant protective agent DIMBOA-Glc.<sup>[7]</sup>

It has been postulated that enzymes of secondary metabolism have evolved through gene duplication from enzymes of primary metabolism.<sup>[8]</sup> In line with this hypothesis, the high sequence identity, as well as structural and functional similarities between the two IGP lyases, suggest that zmTrpA is the progenitor of zmBX1. Based on this hypothesis, we reasoned that it should be possible to remove the zmTrpB1 dependence of zmTrpA by amino acid exchanges that mimic the situation in zmBX1. The resulting stand-alone zmTrpA variant should provide insights into allosteric communication of the TS complex and into the evolutionary relationship between zmTrpA and zmBX1. To identify crucial differences between zmTrpA and zmBX1, we compared the amino acid sequences of the central catalytic  $(\beta\alpha)_8$ -barrel domains, without considering the N-terminal subcellular localization sequences. An initial analysis showed that differences in amino acid sequence were not clustered, but distributed over the whole proteins (Figure S1). We then focused on sequence stretches from loops 2 (residues 56–76) and 6 (residues 178–193 for zmTrpA and residues 174–189 for zmBX1; Figure 1B) because these two loop regions are known to be important for the catalytic activity and allosteric activation of TrpA.<sup>[2,9]</sup> Moreover, both loops together form a lid that covers the active site (Figure 1C). Amino acids in loop 2, which carries one of the two conserved catalytic residues (D62), differ in several positions between zmTrpA and zmBX1. However, these differences seem to be rather insignificant with respect to the physicochemical properties of the corresponding residues (i.e., A61 and V65 in zmTrpA vs. I61 and I65 in zmBX1) or are rather remote from the active site (i.e., Y56 and K76 in zmTrpA vs. C56 and S76 in zmBX1). Loop 6 contains a conserved threonine residue (T184 in zmTrpA, T180 in zmBX1), which is known to form a crucial hydrogen bond with D62.<sup>[9,10]</sup> There are six positions in loop 6 that differ between zmTrpA and zmBX1. The two most prominent ones are T186 in zmTrpA versus P182 in zmBX1 and G192 in zmTrpA versus P188 in zmBX1. In addition, the crystal structure of zmBX1 (PDB ID: 1TJR, chain A) shows a fully resolved loop 6. In contrast, crystal structures of TrpA enzymes display a poorly defined loop 6,

[a] M. Schupfner, Prof. Dr. R. Sterner  
Institute of Biophysics and Physical Biochemistry, University of Regensburg  
Universitätsstraße 31, 93053 Regensburg (Germany)  
E-mail: reinhard.sterner@ur.de

[b] Dr. F. Busch, Prof. Dr. V. H. Wysocki  
Department of Chemistry and Biochemistry and  
Resource for Native Mass Spectrometry Guided Structural Biology  
The Ohio State University  
473 W 12th Ave, Columbus, OH 43210 (USA)

 Supporting information and the ORCID identification numbers for the authors of this article can be found under <https://doi.org/10.1002/cbic.201900323>.

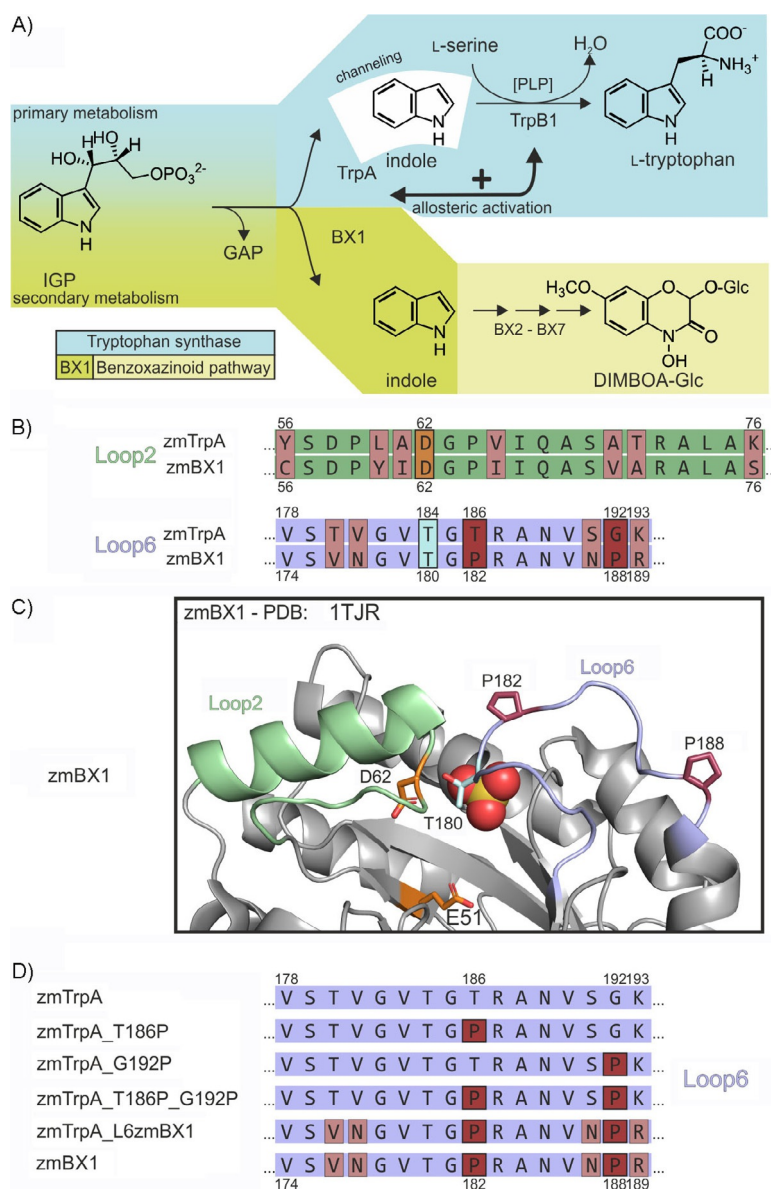


**Figure 1.** A) The cleavage of IGP by the paralogous enzymes TrpA and BX1 in *Z. mays* marks a branch point between primary (tryptophan biosynthesis) and secondary metabolism (benzoxazinoid biosynthesis). In primary metabolism, TrpA is part of the TS and is allosterically activated by the TrpB1 subunit. In secondary metabolism, BX1 is independent of an activating interaction partner.<sup>[7]</sup> B) Sequence comparison of loops 2 and 6 from zmTrpA and zmBX1. In loop 2, the catalytic residue D62 is colored orange. In loop 6, the conserved T184 is colored cyan. The residues that differ between zmTrpA and zmBX1 are colored light red. The positions that carry a proline in zmBX1 are colored dark red. The entire sequences of zmTrpA and zmBX1 are shown in Figure S1. C) Crystal structure of zmBX1 (PDB ID: 1TJR, chain A). Loop 2, consisting of a loop segment and a helical segment is colored green and loop 6 is colored light blue. The proline residues in loop 6 at positions 182 and 188 are colored dark red. The catalytic residues E51 and D62<sup>[5]</sup> are colored orange. Conserved T180 is colored cyan. A sulfate ion, which is represented as a sphere, marks the phosphate-binding pocket at the active site. D) Loop 6 sequences of the experimentally characterized enzymes. For the zmTrpA variants, differences from wild-type zmTrpA are colored dark red (substitutions to proline) or light red (other substitutions).

both in the presence and in the absence of TrpB1. In light of these findings, it has been argued that the higher IGP lyase activity of zmBX1 compared with that of TrpA is based on the stabilization of a specific conformation of loop 6.<sup>[5]</sup> We speculated that the two proline residues in zmBX1 were responsible for this stabilization, and hence, for the increased catalytic activity of zmBX1 compared with that of zmTrpA. To test this hypothesis, we generated the T186P and G192P exchanges in zmTrpA separately and in combination. In addition, we re-

placed the entire loop 6 from zmTrpA with loop 6 from zmBX1 (Figure 1D).

Wild-type and mutant genes were cloned (see Table S1 for mutagenesis primers) and expressed in *Escherichia coli*. The recombinant proteins (Table S2) were purified and analyzed by means of size-exclusion chromatography (SEC) and native MS. In SEC experiments, each of the proteins eluted as a single peak; this indicated a well-defined oligomeric state (Figure S2). MS results showed that zmTrpA and its variants were mono-

mers, and that zmBX1 and zmTrpB1 were dimers (Figures S3, S4). Steady-state enzyme kinetics were recorded for the enzymes zmBX1, zmTrpA, zmTrpA\_T186P, zmTrpA\_G192P, zmTrpA\_T186P\_G192P, and zmTrpA\_L6zmBX1 (Table 1). The determined turnover numbers ( $k_{\text{cat}}$ ) and Michaelis constants for IGP ( $K_{\text{m}}^{\text{IGP}}$ ) of zmBX1 and zmTrpA are comparable to reported

**Table 1.** Steady-state enzyme kinetic parameters for the IGP lyase reaction of zmBX1 and zmTrpA and its variants, in the absence and presence of zmTrpB1.<sup>[a]</sup>

Protein(s)	$k_{\text{cat}}$ [ $\text{s}^{-1}$ ]	$K_{\text{m}}^{\text{IGP}}$ [mM]	$k_{\text{cat}}/K_{\text{m}}^{\text{IGP}}$ [ $\text{M}^{-1}\text{s}^{-1}$ ]
zmBX1	$2.8 \pm 0.1$	$0.005 \pm 0.001$	$5.4 \times 10^5 \pm 9.4 \times 10^4$
zmTrpA	$0.0020 \pm 0.0001$	$0.170 \pm 0.025$	$12 \pm 2.2$
zmTrpA + zmTrpB1	$3.9 \pm 0.1$	$0.175 \pm 0.014$	$2.2 \times 10^4 \pm 2.2 \times 10^3$
zmTrpA_T186P	$0.021 \pm 0.001$	$3.2 \pm 0.3$	$6.5 \pm 8.0 \times 10^{-1}$
zmTrpA_T186P + zmTrpB1	$2.3 \pm 0.1$	$0.043 \pm 0.005$	$5.5 \times 10^4 \pm 7.6 \times 10^3$
zmTrpA_G192P	$0.031 \pm 0.004$	$4.0 \pm 1.2$	$7.7 \pm 3.3$
zmTrpA_G192P + zmTrpB1	$1.34 \pm 0.04$	$0.051 \pm 0.006$	$2.6 \times 10^4 \pm 4.0 \times 10^3$
zmTrpA_T186P_G192P	$0.08 \pm 0.01$	$4.01 \pm 0.75$	$20 \pm 5.2$
zmTrpA_T186P_G192P + zmTrpB1	$2.4 \pm 0.1$	$0.036 \pm 0.006$	$6.8 \times 10^4 \pm 1.4 \times 10^4$
zmTrpA_L6zmBX1	$1.04 \pm 0.05$	$1.8 \pm 0.3$	$5.7 \times 10^2 \pm 1.2 \times 10^2$
zmTrpA_L6zmBX1 + zmTrpB1	$0.46 \pm 0.01$	$0.080 \pm 0.006$	$5.8 \times 10^3 \pm 5.8 \times 10^2$
zmTrpA_T186M	$0.057 \pm 0.001$	$3.9 \pm 0.2$	$15.1 \pm 1.1$
zmTrpA_T186I	$0.024 \pm 0.001$	$3.0 \pm 0.3$	$8.1 \pm 1.1$

[a] Experimental conditions: 100 mM *N*-(2-hydroxyethyl)piperazine-*N'*-(3-propanesulfonic acid (EPPS)/KOH (pH 7.5), 180 mM KCl, 40 mM PLP, 6 mM  $\text{NAD}^+$ , 20 mM  $\text{NaAsO}_4$ , various concentrations of IGP, 100 mM L-serine (in the presence of zmTrpB1), and 5.5  $\mu\text{M}$  GAP dehydrogenase from *Thermotoga maritima*. The reaction was followed at 30 °C by monitoring the cleavage of IGP to GAP and indole with a coupled enzymatic assay.<sup>[14]</sup> The mean and standard error were calculated from at least three independent measurements.

values,<sup>[6b,8c]</sup> with zmBX1 exhibiting a  $k_{\text{cat}}$  ( $2.8 \text{ s}^{-1}$ ) that exceeds the  $k_{\text{cat}}$  of zmTrpA by three orders of magnitude. In comparison to zmTrpA, the  $k_{\text{cat}}$  values of the single mutants zmTrpA\_T186P and zmTrpA\_G192P were enhanced 10- to 15-fold. The  $k_{\text{cat}}$  value of the double mutant zmTrpA\_T186P\_G192P was enhanced 40-fold, whereas the  $k_{\text{cat}}$  value of zmTrpA\_L6zmBX1 was enhanced 520-fold. Thus, the  $k_{\text{cat}}$  value of zmTrpA\_L6zmBX1 is close to those of zmBX1 and zmTrpA in complex with its activating binding partner zmTrpB1. All zmTrpA variants show a significantly enhanced  $k_{\text{cat}}$  value and they display an increased  $K_{\text{m}}^{\text{IGP}}$  value relative to those of zmBX1 and zmTrpA (Table 1). These results demonstrate that the exchanges of T186P and G192P, as well as the incorporation of the whole of loop 6 of zmBX1, are sufficient to accelerate turnover rates for zmTrpA, albeit negatively affecting the binding of the substrate IGP.

We next used SEC and activity titrations to test whether the activated zmTrpA variants were still able to bind zmTrpB1. The results showed that all variants formed a complex with zmTrpB1 (Figure S5). The apparent dissociation constants ( $K_{\text{D}}^{\text{app}}$ ), as determined by measuring TrpA activity as a function of zmTrpB1 concentration, are between 0.3 and 0.7  $\mu\text{M}$ ; these

values are comparable to the  $K_{\text{D}}^{\text{app}}$  value of 0.5  $\mu\text{M}$  for the zmTrpA:zmTrpB1 complex (Table S3). The effect of zmTrpB1 binding on the steady-state kinetic parameters of zmTrpA and its activated variants are summarized in Table 1. Wild-type zmTrpA shows a 2000-fold increased  $k_{\text{cat}}$  value in the presence of zmTrpB1, whereas the  $K_{\text{m}}^{\text{IGP}}$  value is unaffected. The variants zmTrpA\_T186P, zmTrpA\_G192P, and zmTrpA\_T186P\_G192P display 30- to 100-fold improved  $k_{\text{cat}}$  values in the presence of zmTrpB1, whereas the  $K_{\text{m}}^{\text{IGP}}$  values are decreased 70- to 110-fold. Interestingly, the variant zmTrpA\_L6zmBX1 displays a two-fold reduced  $k_{\text{cat}}$  value, whereas the  $K_{\text{m}}^{\text{IGP}}$  value is lowered 20-fold. Apparently, an optimal catalytic activity for zmTrpA is achieved by the exchange of its loop 6 with that of zmBX1 and cannot be further increased by the presence of zmTrpB1. It has been shown for TrpA from *Salmonella typhimurium* that the transition from a rather inactive to a highly active conformation is the rate-limiting step for the IGP lyase reaction.<sup>[11]</sup> This conformational change, which is triggered by the formation of the aminoacrylate intermediate in TrpB1, includes loop 6. It is therefore plausible to assume that zmTrpA\_L6zmBX1 has become independent of zmTrpB1 because loop 6, stemming from zmBX1, constitutively adopts the active conformation. In contrast, substrate binding, as reflected by the  $K_{\text{m}}^{\text{IGP}}$  value, is impaired in the zmTrpA variants. It can, however, be restored to the wild-type level through the interaction with zmTrpB1, for reasons that are unclear at this point.

The improved catalytic activities of the variants zmTrpA\_T186P and zmTrpA\_G192P raised the question whether residues other than proline had a similar activating effect at positions 186 and 192. We therefore tested, at both positions, a set of amino acids that sampled a range of diverse physicochemical properties.<sup>[12]</sup> Mutagenesis at position 186 led to two variants, zmTrpA\_T186M and zmTrpA\_T186I, that displayed increased IGP lyase activity (Figure 2). Comparable to zmTrpA\_T186P, zmTrpA\_T186M and zmTrpA\_T186I show a 10- to 30-fold enhanced  $k_{\text{cat}}$  value, but also a 20-fold increased  $K_{\text{m}}^{\text{IGP}}$  value compared with that of zmTrpA (Table 1). Analytical SEC and MS

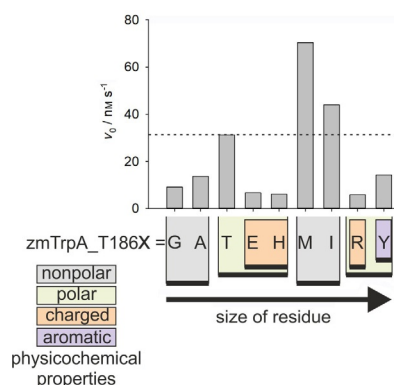


**Figure 2.** Reaction rates of zmTrpA variants with different amino acids at position 186. The dashed line indicates wild-type activity. Experimental conditions: 100 mM EPPS/KOH (pH 7.5), 180 mM KCl, 40 mM PLP, 6 mM  $\text{NAD}^+$ , 20 mM  $\text{NaAsO}_4$ , 5.5  $\mu\text{M}$  GAP dehydrogenase from *T. maritima*, 5  $\mu\text{M}$  zmTrpA variant. The reaction was followed at 30 °C by monitoring the cleavage of 1 mM IGP to GAP and indole with a coupled enzymatic assay.<sup>[14]</sup>

demonstrated that both variants were homogeneous monomers (Figures S2 and S3) that formed a complex with zmTrpB1 (Figure S5). Screening of position 192 identified no activating amino acid exchanges other than G192P.

Our work establishes that zmTrpA can be significantly activated by the exchange of two residues in loop 6 with the corresponding residues of zmBX1. This activating effect is further enhanced if the entire loop 6 of zmTrpA is replaced with loop 6 from zmBX1. Thus, our findings reinforce the importance of loop 6 for the allosteric activation of TrpA by TrpB1.<sup>[2]</sup> However, although the turnover number of zmTrpA\_L6zmBX1 is close to that of zmBX1, the Michaelis constant for IGP is increased by several orders of magnitude. Currently, the structural basis for a weaker substrate affinity of the activated variants is unknown and might result from other sequence differences between zmTrpA and zmBX1.<sup>[6a]</sup> Remarkably, high substrate affinity is restored by the interaction of zmTrpA variants with zmTrpB1; thus illustrating the decoupling of stand-alone activity and allosteric activation.

Based on our experimental findings, we propose a plausible model for the evolution of zmBX1 from a progenitor zmTrpA (Figure 3). In this model, gene duplication allows for the evolution of one copy towards zmBX1, whereas the other copy of zmTrpA maintains its role in the canonical TS. On the route towards zmBX1, initial single exchanges at key positions 186 and 192 in loop 6 would have increased the turnover number. The combination of such activating exchanges plus the accumulation of further substitutions would have led to a complete rearrangement of loop 6, with a further drastic increase of activity. For the final transition from zmTrpA to zmBX1, two major changes in properties were necessary: the improvement of affinity for IGP and the formation of the dimer. It is unclear whether these changes in properties occurred in a stepwise manner or along with the improvement of the  $k_{\text{cat}}$  value. In any case, our model is in accordance with the situation found in extant *Z. mays*. Here, a zmTrpA enzyme is activated by zmTrpB1 in the canonical TS, whereas a zmBX1 enzyme displays a high IGP lyase activity without an interaction partner.

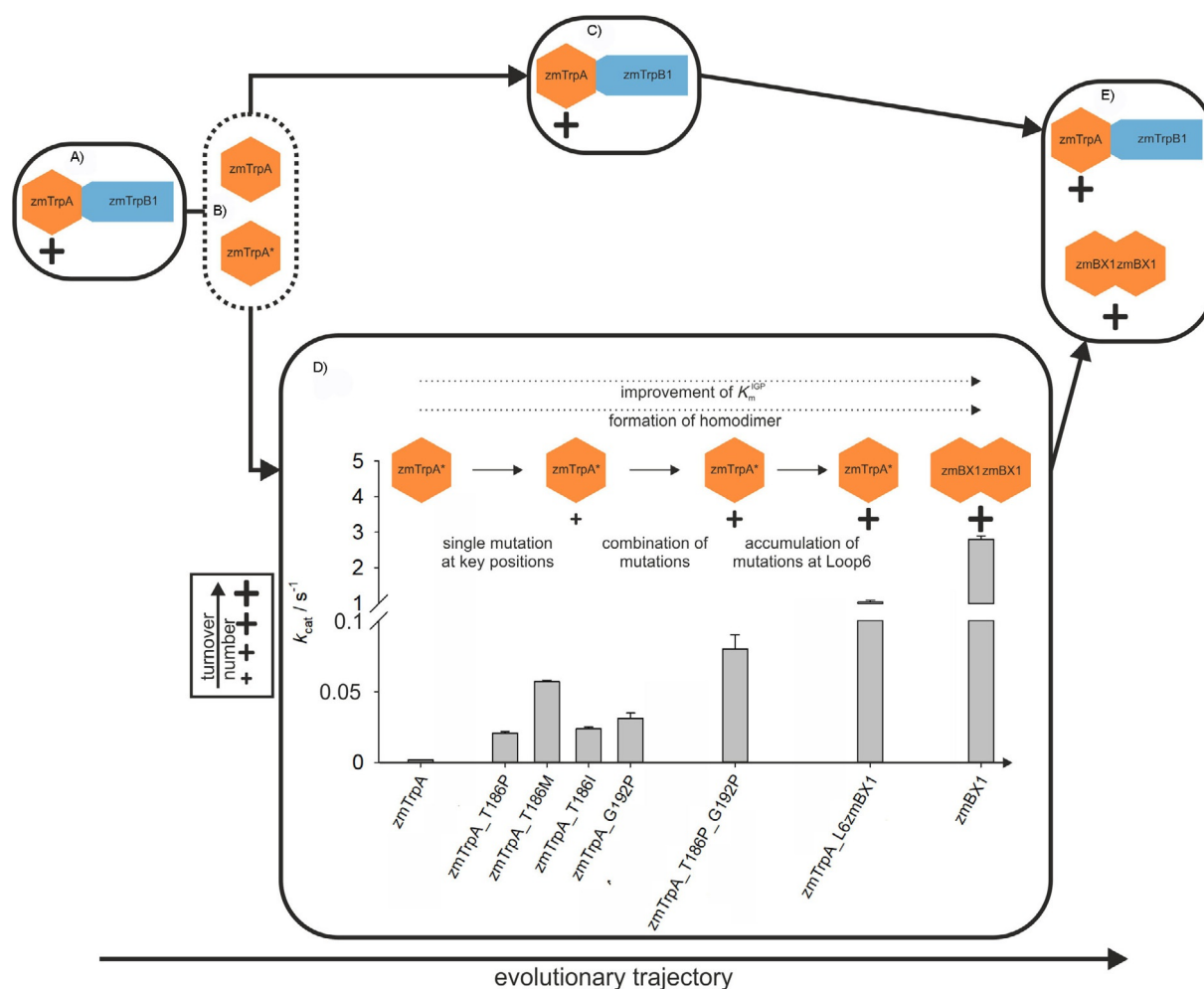


**Figure 3.** Model for the evolution of zmTrpA to zmBX1. The plus sign size indicates the relative IGP lyase activity of the depicted variants. A) Initial situation: TS complex with the IGP lyase activity of zmTrpA being stimulated by zmTrpB1. B) The gene for zmTrpA is duplicated. C) The TS complex remains unaltered, whereas D) zmTrpA\* sequentially accumulates beneficial mutations that enhance its IGP lyase activity towards that of zmBX1. The bars indicate the experimentally determined  $k_{\text{cat}}$  values. Solid arrows describe experimentally confirmed steps, whereas dashed arrows indicate the steps necessary for the final evolution of extant zmBX1. E) Situation in extant *Z. mays*: the TS complex exists in parallel with zmBX1. For the TS complex, only zmTrpA:zmTrpB1 is shown instead of the entire zmTrpA:zmTrpB1:zmTrpA complex.



Taken together, our findings demonstrate that a small number of amino acid exchanges can be sufficient to drive the evolution of an enzyme from primary metabolism into one of secondary metabolism with altered catalytic and regulatory properties.<sup>[13]</sup>

## Acknowledgements

This work was supported by a grant from the Deutsche Forschungsgemeinschaft to R.S. (STE 891/11-1) and a grant from the National Institutes of Health to V.H.W. (NIH P41GM128577). The cDNA of *Z. mays* W22 was a generous donation from Dr. Kevin Begcy (University of Regensburg). We thank Sonja Fuchs, Christiane Endres, and Jeannette Ueckert for expert technical assistance, and Sandra Schlee, Patrick Babinger, and Rainer Merkl for critical reading of the manuscript.

## Conflict of Interest

The authors declare no conflict of interest.

**Keywords:** enzymes · molecular evolution · primary metabolism · protein design · secondary metabolism

- [1] a) R. Merkl, *BMC Evol. Biol.* **2007**, *7*, 59; b) I. P. Crawford, *Bacteriol. Rev.* **1975**, *39*, 87–120.

- [2] M. F. Dunn, *Arch. Biochem. Biophys.* **2012**, *519*, 154–166.  
[3] A. R. Buller, S. Brinkmann-Chen, D. K. Romney, M. Herger, J. Murciano-Calles, F. H. Arnold, *Proc. Natl. Acad. Sci. USA* **2015**, *112*, 14599–14604.  
[4] R. Sterner, B. Höcker, *Chem. Rev.* **2005**, *105*, 4038–4055.  
[5] V. Kulik, E. Hartmann, M. Weyand, M. Frey, A. Gierl, D. Niks, M. F. Dunn, I. Schlichting, *J. Mol. Biol.* **2005**, *352*, 608–620.  
[6] a) M. Frey, C. Stettner, P. W. Pare, E. A. Schmelz, J. H. Tumlinson, A. Gierl, *Proc. Natl. Acad. Sci. USA* **2000**, *97*, 14801–14806; b) V. Kriechbaumer, L. Weigang, A. Fiesselmann, T. Letzel, M. Frey, A. Gierl, E. Glawischnig, *BMC Plant Biol.* **2008**, *8*, 44.  
[7] M. Frey, K. Schullehner, R. Dick, A. Fiesselmann, A. Gierl, *Phytochemistry* **2009**, *70*, 1645–1651.  
[8] a) L. C. Vining, *Gene* **1992**, *115*, 135–140; b) R. D. Firm, C. G. Jones, *Mol. Microbiol.* **2000**, *37*, 989–994; c) M. Frey, P. Chomet, E. Glawischnig, C. Stettner, S. Grun, A. Winklmaier, W. Eisenreich, A. Bacher, R. B. Meeley, S. P. Briggs, K. Simcox, A. Gierl, *Science* **1997**, *277*, 696–699.  
[9] J. M. Axe, K. F. O'Rourke, N. E. Kerstetter, E. M. Yezdimer, Y. M. Chan, A. Chasin, D. D. Boehr, *Protein Sci.* **2015**, *24*, 484–494.  
[10] a) X. J. Yang, E. W. Miles, *J. Biol. Chem.* **1992**, *267*, 7520–7528; b) V. Kulik, M. Weyand, R. Seidel, D. Niks, D. Arac, M. F. Dunn, I. Schlichting, *J. Mol. Biol.* **2002**, *324*, 677–690.  
[11] K. S. Anderson, E. W. Miles, K. A. Johnson, *J. Biol. Chem.* **1991**, *266*, 8020–8033.  
[12] C. Pommié, S. Levadoux, R. Sabatier, G. Lefranc, M. P. Lefranc, *J. Mol. Recognit.* **2004**, *17*, 17–32.  
[13] M. G. Plach, P. Löffler, R. Merkl, R. Sterner, *Angew. Chem. Int. Ed.* **2015**, *54*, 11270–11274; *Angew. Chem.* **2015**, *127*, 11423–11427.  
[14] T. E. Creighton, *Eur. J. Biochem.* **1970**, *13*, 1–10.

Manuscript received: May 14, 2019

Accepted manuscript online: May 15, 2019

Version of record online: August 28, 2019